Binding Model for Nonpeptide Antagonists of $\alpha_v\beta_3$ Integrin

Bradley P. Feuston,*,† J. Chris Culberson,† Mark E. Duggan,‡ George D. Hartman,‡ Chih-Tai Leu,§ and Sevgi B. Rodan§

Departments of Molecular Systems, Medicinal Chemistry and Bone Biology & Osteoporosis Research, Merck Research Laboratories, West Point, Pennsylvania 19486

Received July 19, 2002

A binding model for nonpeptide antagonists of integrin $\alpha_v\beta_3$ has been developed through docking analyses utilizing the MMFFs force field and the recently published crystal structure, 1JV2. Results of this docking study have led to the identification of a novel binding model for selective antagonists of $\alpha_v\beta_3$ over $\alpha_{IIb}\beta_3$ integrins. Four different chemical classes are shown to bind in a similar fashion providing a measure of confidence in the proposed model. All $\alpha_v\beta_3$ and $\alpha_{IIb}\beta_3$ antagonists have a basic nitrogen separated some distance from a carboxylic acid to mimic RGD. For the $\alpha_v\beta_3$ antagonists under present consideration, these charged ends are separated by twelve bonds. The basic nitrogen of the active $\alpha_v\beta_3$ ligands are shown to interact with D150 of α_v and the ligands' carboxylic acid interact with R214 of β_3 while adopting an extended conformation with minimal protein induced internal strain. In addition, an energetically favorable interaction is found with all of the active $\alpha_v\beta_3$ molecules with Y178 of α_v when docked to the crystallographically determined structure. This novel interaction may be characterized as $\pi-\pi$ stacking for the most active of the $\alpha_v\beta_3$ selective antagonists. The proposed model is consistent with observed activity as well as mutagenicity and photoaffinity cross-linking studies of the $\alpha_v\beta_3$ integrin.

Introduction

Integrins are a family of cell surface glycoproteins that are considered pharmaceutical targets in a number of therapeutic areas since they play a crucial role in cell−cell and cell−extracellular matrix interactions. Although integrins have been implicated in a variety of therapies for cancer, macular degeneration, and arthritis among others so far the only anti-integrin therapy has been achieved by targeting the platelet specific integrin $\alpha_{IIb}\beta_3$.[1−3] The vitronectin receptor, $\alpha_v\beta_3$ integrin, which recognizes an RGD peptide sequence in many extracellular proteins, has been identified as a target for osteoporosis. Osteoporosis is a disease characterized by low bone mass where it is thought that the bone resorption cycle exceeds bone formation during normal remodeling of the bone tissue, which goes on throughout life. The maintenance of normal bone mass depends on a tightly coupled process between two types of bone cells: the osteoclasts that resorb bone and the osteoblasts that are responsible for bone formation. An initial step in osteoclastic bone resorption is the adherence of osteoclasts to bone surfaces which is thought to be mediated by $\alpha_v\beta_3$ integrin, expressed in great abundance by the osteoclasts.[4] An antibody to this integrin inhibited bone resorption in vitro, and subsequently the efficacy of this antibody was also demonstrated in an in vivo bone resorption model.[5,6] In addition to the studies with $\alpha_v\beta_3$ antibodies, several studies utilizing either echistatin, an RGD-containing 49 amino acid peptide, RGD peptides or most recently RGD mimetics further demonstrated that $\alpha_v\beta_3$ integrin is a valid target for osteoporosis.[7] Consistent with these findings, the β_3 null mice exhibited mild osteosclerosis due to dysfunctional osteoclasts.[8]

Since the discovery of integrins about 20 years ago, there have been numerous studies on the structure of the integrins. The overall shape and dimensions of integrins have been determined by electron microscopy.[9] Integrin α and β subunits are transmembrane proteins expressed in surface membranes as heterodimers. The extracellular structure of both subunits is best characterized as a large "head" region supported by a long thin tail extending into the transmembrane region with the two heads coming together to form the putative binding site. The head of the α subunits features the so-called β propeller motif, seven homologous blades packed in a cylindrical fan shape, and the ~200 residue "inserted" or I domain (also homologous to the A domain of the von Willebrand factor), therefore called I or A domain. Crystal structures of the A domains (αA) of several integrins have been determined, and an important feature of this domain is the metal-ion-dependent adhesion site (MIDAS).[10] However, the α_v subunit was not predicted to contain this domain while the β_3 subunit was predicted to have an αA-like domain (βA).[11] The existence of a MIDAS motif in β_3 was predicted in a naturally occurring mutation of Y119D in $\alpha_{IIb}\beta_3$ integrin that resulted in abnormal ligand and cation binding functions.[12] Later a MIDAS motif was predicted to occupy the top of the β strand (βA); however, until recently this motif has not been directly demonstrated to bind metal ions.[11] Xiong et al. identified a MIDAS motif in the βA domain of the β_3 subunit when they determined the crystal structure of the extracellular segment of $\alpha_v\beta_3$ integrin in the presence of Ca^{2+}.[13]

* To whom correspondence should be addressed. Tel: (215) 652-5048. Fax: (215) 652-4625. E-mail: bradley_feuston@merck.com.
† Molecular Systems.
‡ Medicinal Chemistry.
§ Bone Biology & Osteoporosis.

10.1021/jm0203130 CCC: $22.00
Published on Web 11/07/2002

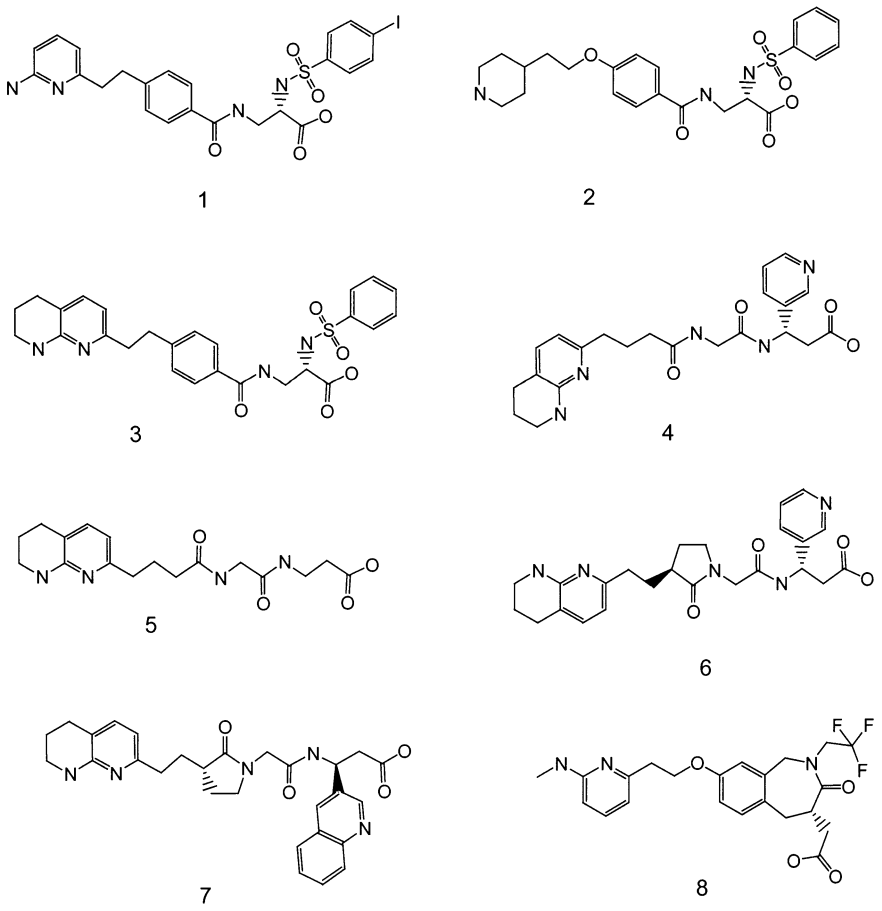

Figure 1. Two-dimensional representation of molecules used in present docking study.

We have previously reported on the design of RGD mimetics as potential antithrombotic ligands targeting the fibrinogen receptor, $\alpha_{IIb}\beta_3$ integrin.[14,15] In general, $\alpha_{IIb}\beta_3$ and $\alpha_v\beta_3$ antagonists are characterized as zwitterionic structures that retain the α-carboxylic acid of aspartic acid and a basic moiety that mimics the arginyl guanidine present in the RGD triad. Previous work from our laboratory demonstrated that potent and selective $\alpha_v\beta_3$ antagonists can be generated from selective fibrinogen receptor ($\alpha_{IIb}\beta_3$) antagonists by the introduction of alternative guanidine replacements at the N-terminus.[16] This effort led to the hypothesis that the N-terminus of an $\alpha_v\beta_3$ antagonist was preferentially interacting with the α_v subunit while the C-terminus interacted with the β_3 subunit. In the absence of any crystal structure for $\alpha_v\beta_3$, neither the binding site nor the bound conformation of any potent small molecule antagonists could be adequately modeled. With the availability of the crystal structure of $\alpha_v\beta_3$ integrin,[13] it became possible to model the binding of small molecule ligands to $\alpha_v\beta_3$ which led to a consistent picture of binding and the focus of the research presented below. Consistent with previous SAR, it is found that the basic nitrogen of the ligand interacts with α_v, in particular D150, while the ligand's acid component interacts with R214 of β_3. In addition, an unexpected finding of $\pi-\pi$ stacking interaction for the "exo-site substituent" with Y178 of α_v, correlates with increased activity and specificity for $\alpha_v\beta_3$.[14]

Ligands. The structures of the ligands, employed in the present effort, are depicted in Figure 1. Molecules **1**−**8** can be divided into four distinct classes. Molecules **1**−**3** belong to the sulfonamide class, **4** and **5** are RGD mimics, and **6** and **7** are constrained glycine amides.[16−18] Molecule **8** is the $\alpha_v\beta_3$ antagonist reported by GlaxoSmithKline as SB 273005.[19] The affinities of these compounds for the $\alpha_v\beta_3$ receptor were determined by a scintillation proximity bead-based binding assay using ^{125}I-labeled **1** as the ligand.[16] In this $\alpha_v\beta_3$ Scintillation Proximity Assay (SPAV3), the $\alpha_v\beta_3$ integrin was purified from HEK 293 cells overexpressing human recombinant $\alpha_v\beta_3$. The method is essentially as described for purification of $\alpha_v\beta_3$ from human placentae by Yamamoto et al.[20] The assay utilizes lyophilized wheat germ agglutinin scintillation proximity beads and has been previously described in detail.[16]

The efficacy of these compounds was also tested in inhibition of platelet aggregation (PLAGGIN assay) since the principal platelet integrin is $\alpha_{IIb}\beta_3$ which shares the same β subunit with $\alpha_v\beta_3$.[16] The assay results for **1**−**8** are shown in Table 1. Molecule **2**, selective for $\alpha_{IIb}\beta_3$, has been included as a negative control for the binding model. In **2**, there are 15 bonds between the carbon atom of the carboxylic acid and the basic nitrogen atom, whereas the similarly charged groups on the $\alpha_v\beta_3$ specific ligands are only separated by twelve bonds. Displacement of ^{125}I-labeled **1** from human recombinant $\alpha_v\beta_3$ (SPAV3 assay) suggests that compounds **1**, **3**−**8** interact with the same sites on the $\alpha_v\beta_3$ receptor. Therefore, any ligand−protein interaction model should account for the binding of these four different chemical classes.

Table 1. Results for Each Molecule in the $\alpha_v\beta_3$ (SPAV3) and $a_{IIb}\beta_3$ (PLAGGIN) Binding Assays

		IC_{50}	
molecule ID	class	SPAV3 (nM)	PLAGGIN (nM)
1	sulfonamide	0.08	1600
2	sulfonamide	>1000	10
3	sulfonamide	0.07	260
4	glycine-containing	8.8	>10000
5	glycine-containing	111	>10000
6	glycine-constrained	0.35	>10000
7	glycine-constrained	0.04	776
8	benzazepine	0.15	>10000

Modeling. When a crystal structure or high quality homology model can be constructed, the first step in a modeling experiment is to produce a model of how the small molecule of interest and the protein interact. These models provide a better understanding of the important residue interactions and assist in the identification of specific regions of the small molecule suitable for modification during lead optimization. The primary objective from a modeling perspective is to provide knowledge and insight for the fast development of potent and selective drugs. Research efforts to optimize lead compounds, i.e., modify lead compound structure for optimum binding and pharmakinetics properties, are directly impacted by these modeling efforts. To obtain useful models of the small molecule and protein interactions, the conformational space of the ligand and possibly the protein are sampled. The binding energy between ligand and protein, determined by the sum of intramolecular energies of the ligand and protein and the intermolecular interaction energy between the ligand and the protein, is employed as a yardstick to evaluate the validity of the model. Models that yield good intermolecular interactions without creating significant internal molecular strain are considered more plausible. Internal strain is directly measured from deviations from normal bond lengths, bond angles, and torsion angles. In addition to energetic considerations, models that were consistent with the results of both natural mutations and mutagenesis of the subunits as well as photoaffinity cross-linking studies on the $\alpha_v\beta_3$ integrins were also favored in the present effort.[12,21−23]

Since the discovery of the integrins, substantial amounts of data have accumulated regarding the location of potential ligand binding sites. The earliest identification of the ligand sites was achieved using the platelet integrin $\alpha_{IIb}\beta_3$.[24] Initially, several naturally occurring mutations in the β_3 subunit which cause Glanzmann thrombasthenia, a severe bleeding disorder, were useful in the identification of these binding sites. Two of the naturally occurring mutations are in the putative βA domain, D145Y and D145N.[12,23] In individuals who have the D145Y mutation, the platelet $\alpha_{IIb}\beta_3$ levels were almost normal but the ability to bind the natural ligand fibrinogen was lost. Importance of the R214 residue in the β_3 subunit was established by binding studies utilizing peptides or antibodies corresponding to the 211−222 residues which was also confirmed by natural mutations at R214 in β_3.[25−27] Previous cross-linking studies with RGD ligands using either $\alpha_{IIb}\beta_3$ or $\alpha_v\beta_3$ integrins not only established that the α and β subunits had to be in close proximity for binding, but also defined the regions of binding in each subunit.[12,21] More recently, Scheiber et al. showed that the C-terminus of echistatin (an RGD-containing 49 amino acid peptide) could also be cross-linked to the region spanned by residues 209−220 of the β_3 subunit.[28] Using these results as well as structure−activity relationship that was developed through in-house research, a large region between the α_v and β_3 subunits was targeted as the potential docking site.

Figure 2. Interfacial region between α_v (yellow) and β_3 (green) "heads". Residues colored red indicate the putative binding region.

Initially both in-house and third party docking software was utilized in the search for specific ligand binding sites within the larger targeted region. In Figure 2, a 3D picture of the "head-to-head" interfacial region of the α_v and β_3 subunits is shown with the axis of the cylindrical motif of the seven β propellers of the α_v subunit lying horizontally. There are four calcium atoms shown at the bottom of the β propellers and another associated with the MIDAS site in β_3. The general region of the putative binding site is also depicted in Figure 2, where residues 145−154 and 212−220 are colored red for α_v and β_3, respectively. The problems encountered in the automated docking calculations are exemplified by FLOG, Merck's in-house docking program.[29] This method relies on a database of precomputed conformations for sampling the 3D conformational space. For these studies a database of 100 conformations with a root-mean-square-deviation (RMSD) of at least 0.6/ between each conformation was generated using the knowledge-based program *et* for each of the candidate ligands.[30] Using a grid generated for the interface region, each conformation was docked and scored based upon overlap of desired properties, e.g., H-bond donor, H-bond acceptor, polar, hydrophobic, and van der Waals interactions. It was found that treating our highly charged ligands as H-bond acceptors or donors was inappropriate resulting in docked conforma-

tions dominated by hydrophobic and van der Waals interactions. Similar to the results of FLOG, the third party docking programs were also found to treat charged interactions poorly.

Since suitable binding conformations that were consistent with experimental data that accounted for the charged nature of the ligand were not identified, it was decided to dock the ligands by hand. In this controlled docking procedure the ligand is placed into a reasonable position and then energy-minimized. From the crystal structure and the mutagenicity data, it seemed plausible that D148 or D150 in α_v interacted with N-terminus while R214 (β_3) interacted with the C-terminus of the ligand.

Molecule **1** served as the reference for all binding models since it was the displacement of this radioligand that was measured in the SPAV3 assay.[16] Using multiple conformations of **1**, it was found that D148/D150 (α_v) and R214 (β_3) were at the appropriate distance to accommodate an extended conformation. Using a hand-generated conformation of **1** placed in a reasonable binding orientation, protein atoms within 10.0Å of the ligand were identified as the binding site. The ligand was then energy minimized in the binding site using formal charges of +1 on the N in the pyridine and −1 on the O of the carboxylic acid using the MMFFs force field in BATCHMIN with a dielectric constant of 1.0.[31,32] Protein atoms were initially held fixed at their crystallographically determined positions. The resultant ligand conformation was then minimized in the absence of the protein to remove protein−ligand interaction induced strain in the conformation. This second relaxation was performed for the neutral molecule using the 4r distance dependent dielectric constant. Energy minimization of the fully charged ligand in a vacuum would bring the two charged ends together to form a cupped conformation. This relaxed conformation, complete with formal charges, was placed back into the binding site and minimized once again in the presence of the protein. The conformational space of the ligands was sampled using the conformation generator *et*.[30] Using these initial conformations combined with manual rotation of torsion angles to overcome local minima, the docking procedure was repeated many times for each of the ligands in an attempt to find a ligand conformation with the least internal strain and the best protein−ligand binding interactions. The protein atoms, specifying the active site, were redefined using the best binding mode of **1** identified as discussed above. Insignificant changes in the protein−**1** interaction occurred when **1** was minimized in this redefined site. The binding site (Figure 3), defined for **1**, was then utilized for the remaining ligands. The residues, which define the binding site, are given in Table 2. It is interesting to note that the β_3 subunit contributes twice as many residues to the binding site than α_v, although as discussed below, α_v seems to be more important for selectivity of the $\alpha_v\beta_3$ ligands.

Having identified the best binding mode for each of the ligands in the rigid crystal structure, the side-chain atoms of the protein within 5 Å of the ligand were permitted to relax along with the ligand. In this final energy minimization procedure, all the protein backbone atoms and the side-chain atoms beyond 5 Å of the docked ligand remained in fixed positions.

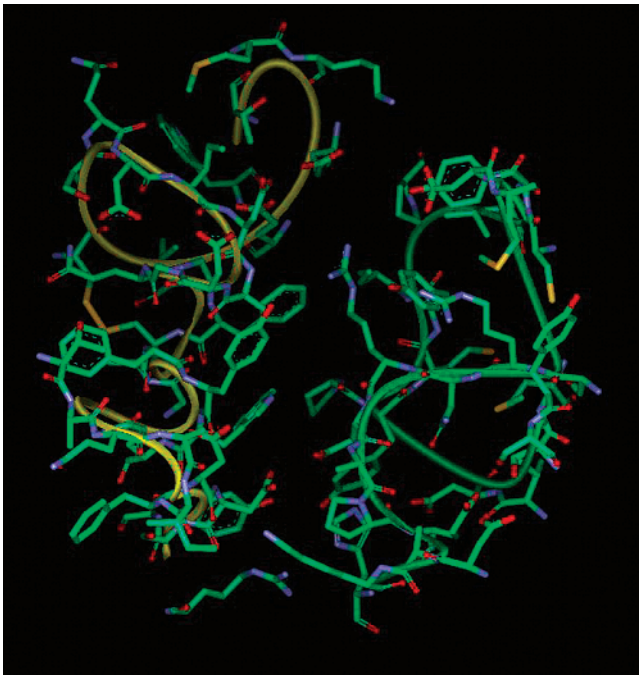

Figure 3. Binding site as defined in present model.

Table 2. Residue Numbers Identified in the Putative Binding Site

subunit	total residue count	residues in binding site
α_v	24	114, 116−123, 145−154, 177−179, 218, 219
β_3	50	119−127,156−158, 163, 164, 166, 167, 169, 170, 173, 177, 180, 182, 184, 187, 212−220, 250−254, 310−314, 318, 333−336

Table 3. Root-Mean-Square Deviations: Minimum RMSD between Bound Conformations and Conformation of Closest Energy Minimum[a]

molecule ID	RMSD (Å): minimum	RMSD (Å): side chain	RMSD (Å): flex-conformational	RMSD (Å): flex-absolute position
1	1.19	0.49	0.54	1.41
2	0.98	0.66	1.10	5.44
3	1.00	0.57	0.77	2.49
4	1.15	0.49	0.46	0.75
5	1.15	0.47	1.25	2.28
6	0.92	0.47	0.71	0.95
7	0.97	0.59	0.89	2.94
8	1.12	0.59	0.41	2.55

[a] Side chain: RMSD of protein atoms before and after relaxation. Conformational: RMSD between small molecule bound conformations in rigid and relaxed protein after overlay. Absolute position: RMSD between small molecule conformations in rigid and relaxed protein using 3D coordinates.

Results and Discussion

In Table 3, the root-mean-square-deviation (RMSD) are given for a number of ligand−ligand and protein−protein comparisons. Column 2 (minimum) contains the RMSD between the bound conformation and conformation corresponding to the closest local energy minimum identified in vacuo for the neutral molecule. Since the closest minimum is not always achieved simply by minimizing the bound conformation in vacuo, 350 conformations were enumerated using the conformation generator *et*, followed by energy minimization with

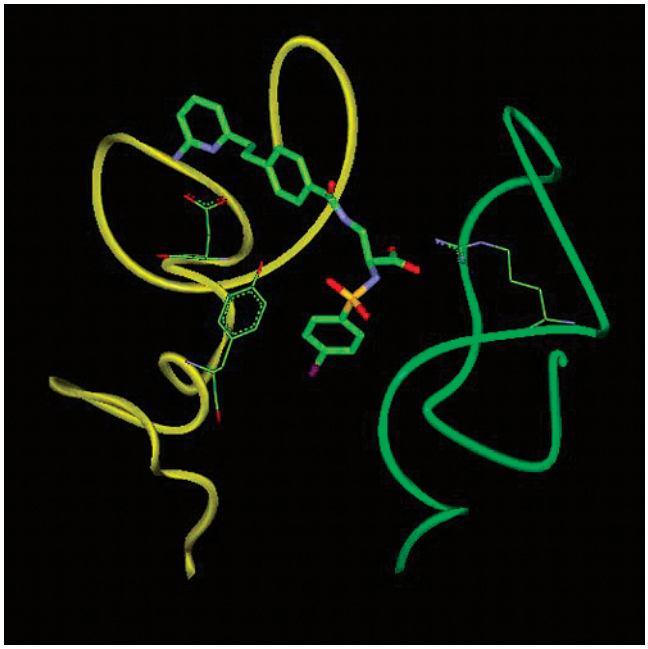

Figure 4. Binding mode for molecule **1**. Protein atoms in crystallographically determined positions.

Figure 5. Binding mode for molecule **2**. Protein atoms in crystallographically determined positions.

Figure 6. Binding mode for molecule **3**. Protein atoms in crystallographically determined positions.

MMFFs. The isolated ligands were treated as formally neutral and minimized using the 4r distance dependent dielectric. The conformation in this set of energy minimized structures with the lowest RMSD to the bound conformation was identified and the RMSD reported in column 2 (minimum) of Table 3. This RMSD is an indication of the internal strain induced in the ligand due to the protein interaction. Since all RMSD's are small, less than 1.2 Å, it is apparent that the molecules have not accumulated significant internal strain. The RMSD between the crystal structure of the protein binding site and the binding site obtained by relaxing the nearest side-chains to the bound ligand is given in column 3 (side chain). Since only side-chain atoms, within 5 Å of the ligand, were allowed to relax while the remaining side-chain and main-chain atoms were held fixed, it is not surprising that these RMSD values are low. Interestingly, the ligands relax concurrently with the side-chain atoms as shown in columns 4 and 5 of Table 3. Column 4 (flex-conformation) is the RMSD between the original crystal docked conformation and the relaxed docked conformation when superimposed, while column 5 (absolute position) is the RMSD between the two docked conformations, calculated using the actual 3D coordinates. Differences in the binding modes for the various ligands are more clearly manifested in these last two RMSD analyses and by visualization of the corresponding docked ligand.

The binding models for ligands with the crystal structure are shown in Figures 4−11, for **1**−**8**, respectively. The protein binding site, as depicted in Figure 3, is now shown primarily in ribbons with α_v colored yellow and β_3 in green. In addition, three residues, D150 and Y178 of α_v and R214 of β_3, that are found to play an important role in selective $\alpha_v\beta_3$ binding are displayed in stick mode. The ligand−protein interaction distances for these three $\alpha_v\beta_3$ protein's residues are listed in Table 4 before and after the protein relaxation. The distances given in Table 4 are for the nearest ligand-residue heavy atom separation and help characterize the binding site.

The basic nitrogen terminus of **1** interacts with D150 in α_v while the carboxylic acid binds to R214 in β_3 as seen in Figure 4 and Table 4. The molecule has an extended conformation and only makes a slight readjustment when the side chains are allowed to relax as indicated in columns 4 and 5 and seen in Figure 12. In Figure 12, the solid-colored conformation is obtained after relaxing the side chains. The same ligand−protein interactions are maintained as with the crystal structure before relaxing the side chains. A new unexpected

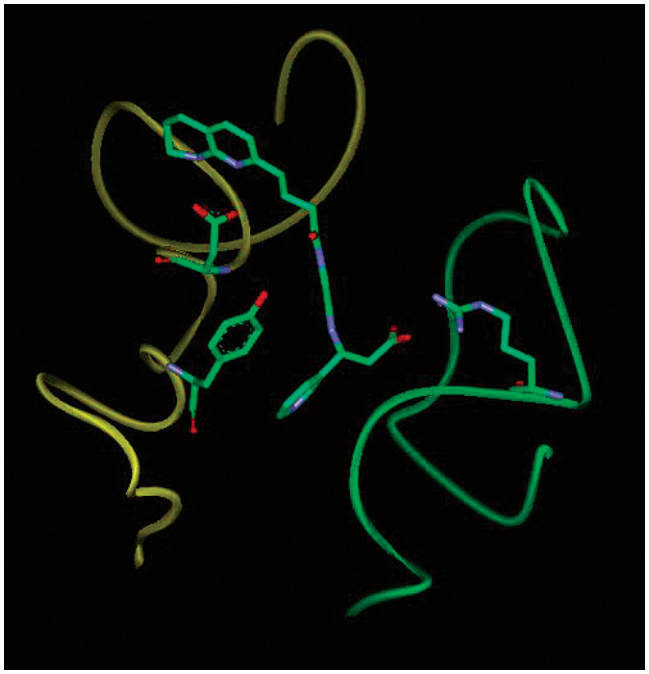

Figure 7. Binding mode for molecule **4**. Protein atoms in crystallographically determined positions.

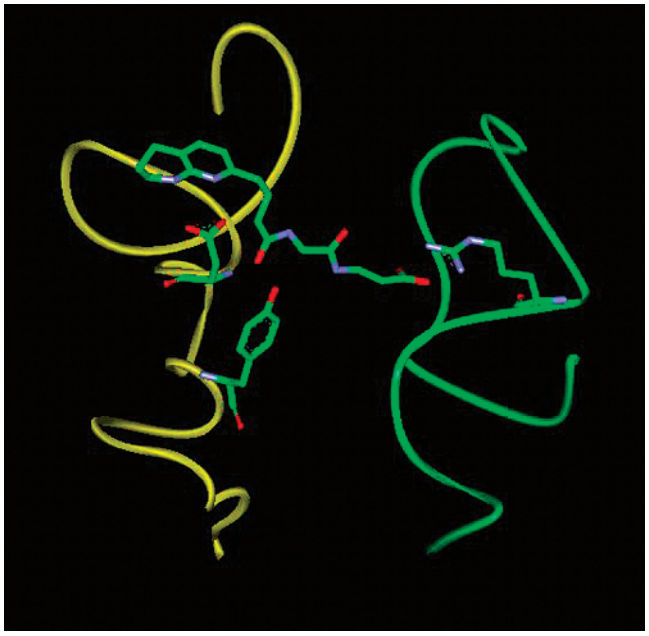

Figure 8. Binding mode for molecule **5**. Protein atoms in crystallographically determined positions.

interaction is also depicted in Figure 4, namely a $\pi-\pi$ stacking interaction between Y178 of α_v and the phenol adjacent to the sulfonamide of **1**.[33] This interaction, previously identified as an "exo-site interaction",[14] is treated as a hydrophobic contribution to binding energy by MMFFs and is also observed in the binding modes of **2**, **3**, **4**, **6**, and **7**. The shortest distance between heavy atoms of these ligands and Y178 range from 3.7 Å to 4.6 Å, consistent with a $\pi-\pi$ stacking interaction. Molecule **5**, which lacks the aromatic side chain, is found to interact with Y178 through a hydrogen bond acceptor. Molecule **7** also makes a similar hydrogen bond in addition to the $\pi-\pi$ stacking interaction. All eight ligands interact in fashion similar to the charged

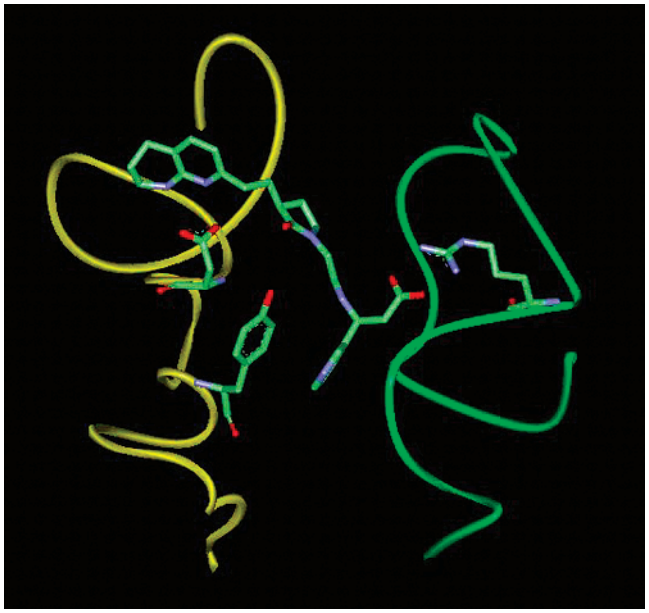

Figure 9. Binding mode for molecule **6**. Protein atoms in crystallographically determined positions.

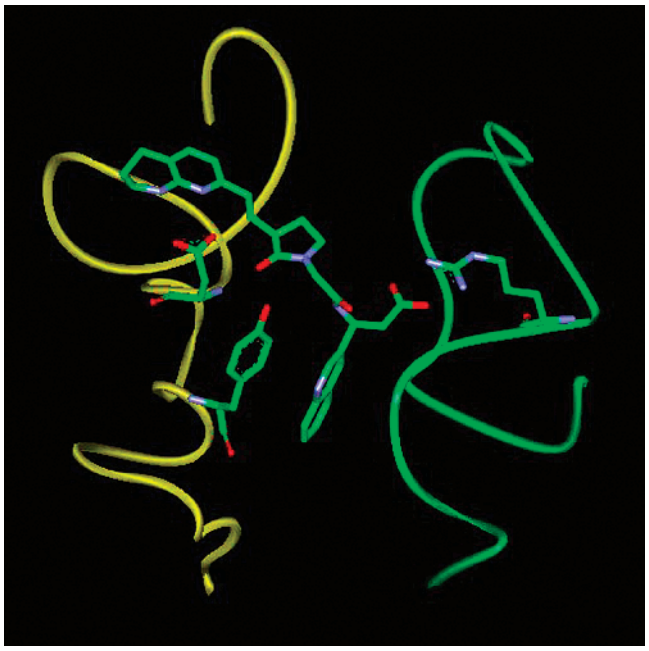

Figure 10. Binding mode for molecule **7**. Protein atoms in crystallographically determined positions.

residues D150 (α_v) and R214(β_3). All adopt an extended conformation, except **2**, which is forced into a cupped conformation to make these contacts. Recall **2**, included as a counter example, is not an antagonist of $\alpha_v\beta_3$ and should not bind as the other ligands. When the side chains of the binding site of **2** are allowed to relax, **2** moves the most of any of the ligands as indicated in column 5 of Table 3 and Figure 13. In fact, **2** is the only ligand to change contacts. Instead of interacting solely with D150, the N-terminus of **2** interaction is equally shared between D150 and D148, with D148 further away from R214 than D150 as indicated in Table 4. Also the interaction with Y178 is completely lost. Due to rotational barriers it would not be expected that **2** could change from a cupped to extended conformation during this energy minimization. Attempts to dock extended

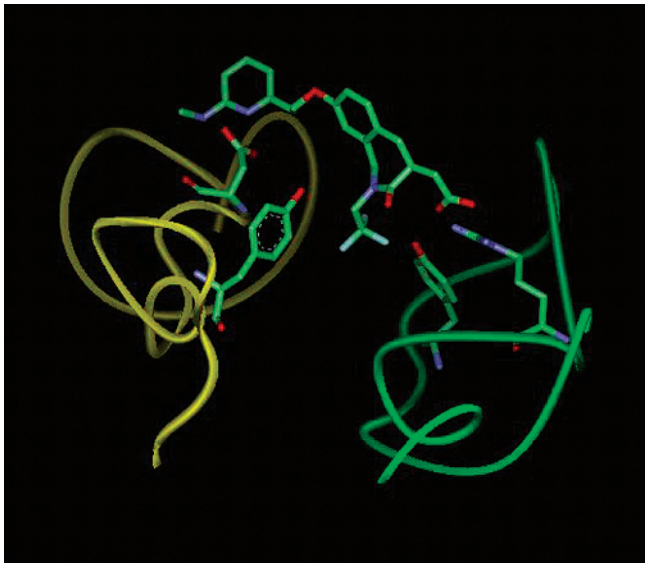

Figure 11. Binding mode for molecule **8**. Protein atoms in crystallographically determined positions.

Table 4. Important Protein−Small Molecule Contact Distances

	contacts in crystal binding site			contacts in relaxed binding site		
molecule ID	R214, Å	D150, Å	Y178,[a] Å	R214, Å	D150, Å	Y178,[a] Å
1	2.5	2.5	3.7 (1)	2.5	2.4	4.0 (1)
2	2.5	2.5	4.6 (1)	2.6	2.6[b]	12.0 (4)
3	2.5	2.5	3.7 (1)	2.5	2.4	4.5 (1)
4	2.7	2.4	3.7 (1)	2.5	2.5	3.9 (1)
5	2.4	2.4	2.8 (2)	2.5	2.6	2.7 (2)
6	2.4	2.4	3.6 (1)	2.5	2.4	3.5 (1, 2)
7	2.5	2.4	3.9 (1, 2)	2.5	3.0	5.0 (1, 2)
8	2.4	2.5	3.8 (3)	2.4	2.4	4.8[c] (3)

[a] Binding type: (1) $\pi-\pi$ stacking; (2) H-bond acceptor; (3) hydrophobic; (4) no binding interaction. [b] Shared with D148 at 2.5 Å. [c] Hydrophobic interaction with Y166 in β_3 at 3.6 Å.

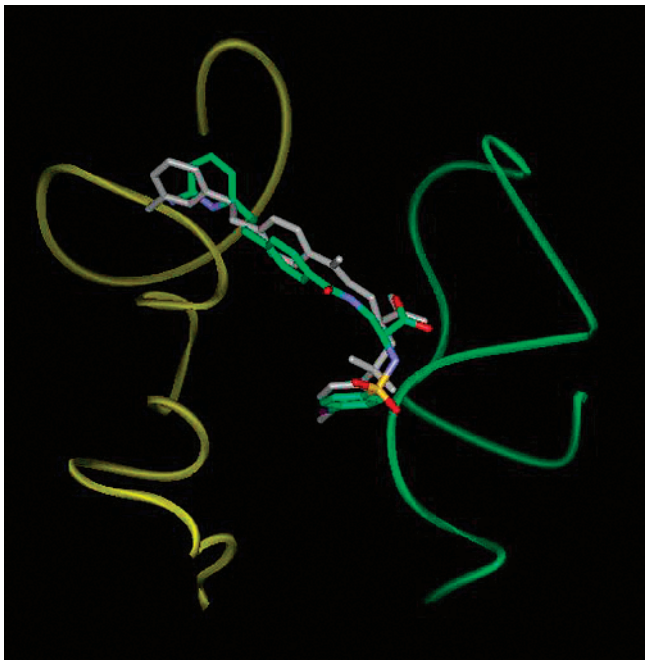

Figure 12. Binding modes for molecule **1** before (green) and after (gray) protein side-chain relaxation.

conformations of **2** in the crystal structure failed because of the relatively long separation between the charged ends.

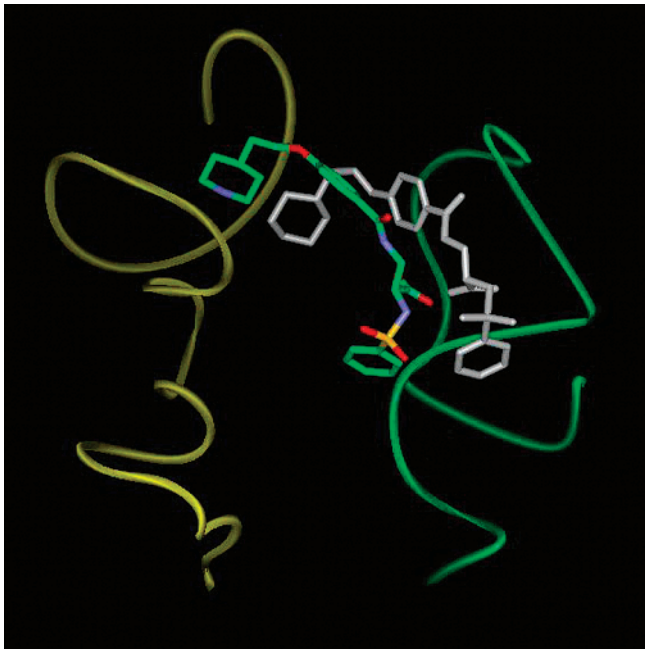

Figure 13. Binding modes for molecule **2** before (green) and after (gray) protein side-chain relaxation.

Molecule **5** is also of interest since it does not have the side groups to make $\pi-\pi$ stacking interaction with Y178 and is the weakest antagonist considered here, with a SPAV3 binding energy more than 4 orders of magnitude greater than that of **1**. However, in Figure 8, a hydrogen bond between the carbonyl on the ligand backbone to the phenyl oxygen on Y178 can be observed. The bound conformation of **5** is also an extended conformation, without significant internal strain and maintains the three primary protein interactions with D150, Y178, and R214 after relaxation (see Tables 3 and 4).

Molecule **8**, similar to **5**, also does not have a $\pi-\pi$ stacking interaction with Y178. However, close examination of the binding mode for **8** revels that the trifluoro group is within 3.8 Å of Y178 and Y166 of α_v and β_3, respectively. The binding of **8** is depicted in Figure 11, where both tyrosines are shown explicitly. In the Protein Data Bank there are multiple examples of trifluoromethyl groups making similar hydrophobic contacts with either a phenylalanine or a tyrosine as in the present model, e.g., 1A29, 1CX2, 1G4P. From these considerations, it is apparent that **8** is making an energetically favorable interaction with Y178 as well. This hydrophobic interaction, shared between the two tyrosines, is also maintained after relaxation of the protein side chains.

The molecules not addressed directly above, **3**, **4**, **6**, and **7**, representing the sulfonamide, glycine-unconstrained, and glycine-constrained chemical classes, are found to dock in a manner consistent with the binding model. From Figures 6, 7, 9, and 10 an extended conformation is depicted for each of these molecules. Analysis of the binding conformations and protein−ligand interactions for these $\alpha_v\beta_3$ specific antagonists show little protein-induced molecular strain while making charged interactions with D150 and R214 and $\pi-\pi$ stacking interaction with Y178.

Conclusions

A model of the preferential binding of nonpeptide ligands to the integrin $\alpha_v\beta_3$ over $\alpha_{IIb}\beta_3$ was developed. The binding mode of these selective antagonists provides a consistent model for the four different chemical classes investigated. Results of docking analyses led to the identification of a novel binding interaction for selective antagonists of the $\alpha_v\beta_3$ integrin. Four different chemical classes are shown to bind in a similar fashion providing a measure of confidence in the proposed model. All seven of the $\alpha_v\beta_3$ antagonists examined have a basic nitrogen interacting with D150 of α_v and a carboxylic acid interacting with R214 of β_3. Also, they all adopt an extended conformation with little ligand−protein-induced internal strain. All of the active molecules (**1**, **3**, **4**, **5**, **6**, **7**, and **8**) have an additional energetically favorable "exo-site" interaction with Y178 of α_v when docked to the crystallographically determined structure. Molecule **2**, a selective antagonist of the fibrinogen receptor, $\alpha_{IIb}\beta_3$, is found to be inactive in the SPAV3 assay and is shown not to fit the binding model since it must adopt a less favorable cupped conformation to make the necessary contacts. Upon protein side-chain relaxation, **2** is expelled from the binding site and only maintains the original C-terminus interaction with R214 of β_3 while the N-terminus shares a charged interaction with D150 and D148 of α_v.

The crystal structure of the extracellular segment of integrin $\alpha_v\beta_3$ complexed to an RGD ligand, elucidated by Xiong et al., confirmed the findings of the earlier studies that the ligand binds at the interface between the two subunits.[34] The arginyl guanidinium group bound by a bidentate salt bridge to D218 and to D150 and the carboxyl group of aspartic acid was in contact with R214. In addition, a recent communication by Gottschalk et al. identified the general binding region of the basic terminus of their ligand as D148 and Y178.[35] Taken together, the proposed model is consistent not only with observed activity as well as mutagenicity and photoaffinity cross-linking studies of the $\alpha_v\beta_3$ integrin but with these recently published results.

Acknowledgment. The authors would like to thank the Merck West Point medicinal chemists whose creativity and dedication have made this work possible.

References

(1) Curley G. P.; Blum H.; Humphries M. J. Integrin antagonists *Cell Mol. Life Sci*. **1999**, *56*, 427−441.
(2) Coller B. S. Perspective Series: Cell adhesion in vascular biology. *J. Clin. Invest.* **1997**, *99*, 1467−1471.
(3) Scarborough, R. M.; Gretler, D. D. Platelet Glycoprotein IIb-IIIa Antagonists as Prototypical Integrin Blockers: Novel Parenteral and Potential Oral Antithrombotic Agents. *J. Med. Chem*. **2000**, *43*, 3453−3473.
(4) Rodan, S. B.; Rodan, G. A. Integrin function in osteoclasts. *J. Endocrinol.* **1997** *154*, S47−S56.
(5) Chambers, T. J.; Fuller, K.; Darby, J. A.; Pringel, J. A. S.; Horton, M. A.; Monoclonal antibodies against osteoclasts inhibit bone resorption in vitro. *Bone Miner*. **1986**, *1*, 127−135.
(6) Crippes, B. A.; Engleman, V. W.; Settle, S. L.; Delarco, J.; Ornberg, R. L.; Helfrich, M. H.; Horton, M. A.; Nickols, G. A. Antibody to β_3 integrin inhibits osteoclast-mediated bone resorption in the thyroparathyroidectomized rat. *Endocrinology* **1996**, *137*, 918−924.
(7) Duong, L. T.; Rodan, G. A. Regulation of osteoclast formation and function. *Rev. Endocrinol. Metab. Dis.* **2001**, *2*, 95−104.
(8) McHugh, K. P.; Hodival-Dilke, K.; Zheng, M.−H.; Namba, N.; Lam, J.; Novack, D.; Fang, X.; Ross, H. P.; Hynes, R.; Teitelbaum, S. L. Mice lacking beta 3 integrins are osteosclerotic due to dysfunctional osteoclasts. *J. Clin. Invest.* **2000**, *105*, 433−40.
(9) Humphries, M. J.; Integrin Structure. *Biochem. Soc. Trans.* **2002**, *28*, 311−339.
(10) Michishita, M.; Videm, V.; Arnaout, M. A. A novel divalent cation-binding site in the A domain of the beta 2 integrin CR3 (CD11b/CD18) is essential for ligand binding. *Cell* **1993**, *72*, 857−867.
(11) Lee, J. O.; Rieu, P.; Arnaout, M. A.; Liddington, R. Crystal structure of the A domain from the alpha subunit of integrin CR3 (CD11b/CD18). *Cell* **1995**, *80*, 631−638.
(12) Loftus, J. C.; O'Toole, T. E.; Plow, E. F.; Glass, A.; Frelinger, A. L., III; Ginsberg, M. H. A beta 3 integrin mutation abolishes ligand binding and alters divalent cation-dependent conformation. *Science* **1990**, *249*, 915−918.
(13) Xiong, J.-P.; Stehe, T.; Diefenbach, B.; Zhang, R.; Dunker, R.; Scott, D. L.; Joachimiak, A.; Goodman, S. L.; Arnaout, M. A.; Crystal Structure of the Extracellular Segment of Integrin $\alpha V\beta 3$. *Science* **2001**, *294*, 339−345.
(14) Hartman, G. D.; Egbertson, M. S.; Halczenko, W.; Laswell, W.; Duggan, M. E.; Smith, R. L.; Naylor, A. M.; Manno, P. D.; Lynch, R. J.; Zhang, G.; Chang, C. T.-C.; Gould, R. L. Nonpeptide Fibrinogen Receptor Antagonists. 1. Discovery And Design of Exosite Inhibitors. *J. Med. Chem*. **1992**, *35*, 4640−4642.
(15) Askew, B. C.; Bednar, R. A.; Bednar, B.; Claremon, D. A.; Cook, J. J.; McIntyre, C. J.; Hunt, C. A.; Gould, R. J.; Lynch, R. J.; Lynch, J. J.; Gaul, S. L.; Stranieri, M. T.; Sitko, G. R.; Holahan, M. A.; Glass, J. D.; Hamill, T.; Gorham, L. M.; Prueksaritanont, T.; Baldwin, J. J.; Hartman, G. D. Non-Peptide Glycoprotein IIb/IIIa INhibitors. 17. Design And Synthesis Of Orally Active, Long-acting Non-peptide Fibrinogen Receptor Antagonists. *J. Med. Chem*. **1997**, *40*, 1779−1788.
(16) Duggan, M. E.; Duong, L. T.; Fisher, J. E.; Hamill, T. G.; Hoffman, W. F.; Huff, J. R.; Ihle, N. C.; Leu, C.-T.; Nagy, R. M.; Perkins, J. J.; Rodan, S. B.; Wesolowski, G.; Whitman, D. B.; Zartman, A. E.; Rodan, G. A.; Hartman, G. D.; Nonpeptide $\alpha_v\beta_3$ Antagonist. 1. Transformation of a Potent, Integrin-Selective $\alpha_{IIb}\beta_3$ Antagonist into a Potent $\alpha_v\beta_3$ Antagonist. *J. Med. Chem*. **2000**, *43*, 3736−3745.
(17) Meissner, R. S.; Perkins, J. J.; Duong, L. T.; Hartman, G. D.; Hoffman, W. F.; Huff, J. R.; Ihle, N. C.; Leu, C.-T.; Nagy, R. M.; Naylor-Olsen, A.; Rodan, G. A.; Rodan, S. B.; Whitman, D. B.; Wesolowski, G.; Duggan, M. E.; Nonpeptide $\alpha_v\beta_3$ Antagonist. 2. Constrained Glycyl Amides Derived From RGD Tripeptide. *Bioorg. Med. Chem. Lett*. **2002**, *12*, 25−29.
(18) Coleman, P. J.; Brashear, K. M.; Hunt, C. A.; Hoffman, W. F.; Hutchinson, J.; Breslin, M. J.; McVean, C. A.; Askew, B. C.; Hartman, G. D.; Rodan, S. B.; Rodan, G. A.; Leu, C.-T.; Prueksaritanont, T.; Fernandez-Metzler, C.; Ma, B.; Libby, L. A.; Merkle, K. M.; Stump, G. L.; Wallace, A. A.; Lynch, J. J.; Lynch, R.; Duggan· M. E. Non-Peptide $\alpha_v\beta_3$ Antagonists. Part III: Identification of Potent RGD Mimetics Incorporating Novel β-Amino Acids as Aspartic Acid Replacements. *Bioorg. Med. Chem. Lett*. **2002**, *12*, 31−34.
(19) Badger, A. M.; Blake, S.; Kapadia, R.; Sarkar, S.; Levin, J.; Swift, B. A.; Hoffman, S. J.; Stroup, G. W.; Miller, W. H.; Gowen, M.; Lark, M. W.; Disease-Modifying Activity of SB273005, an Orally Active, Nonpeptide $\alpha_v\beta_3$ (Vitronectin Receptor) Antagonist, in Rat Adjuvant-Induced Arthritis, *Arthritis Rheum*. **2001**, *44*, 128−137.
(20) Yamamoto, M.; Fisher, J. E.; Gentile, M.; Seedor, J. G.; Leu, C−T.; Rodan, S. B.; Rodan, G. A. The integrin ligand echistatin prevents bone loss in ovariectomized mice and rats. *Endocrinology* **1998**, *139*, 1411−1419.
(21) Smith, J. W.; Cheresh, D. A.; The Arg-Gly-Asp binding domain of the vitronectin receptor. Photoaffinity cross-linking implicates amino acid residues 61−203 of the beta subunit. *J. Biol. Chem*. **1988**, *263*, 18726−18731.
(22) D'Souza, S. E.; Ginsberg, M. H.; Lam, S. C.; Plow, E. F. Chemical cross-linking of arginyl-glycyl-aspartic acid peptides to an adhesion receptor on platelets. *J. Biol. Chem*. **1988**, *263*, 3943−3951.
(23) French, D. L.; Coller, B. S. Haematologically important mutations: Glanzmann thrombasthenia. *Blood Cells Mol. Dis.* **1997**, *23*, 39−51.
(24) Loftus, J. C.; Halloran, C. E.; Ginsberg, M. H.; Feigen, L. P.; Zablocki, J. A.; Smith, J. W. The amino-terminal one-third of alpha Iib defines the ligand recognition specifity of integrin alpha IIb beta 3. *J. Biol. Chem*. **1996**, *271*, 2033−2039.
(25) Charo, I. F.; Nannizzi, L.; Philips, D. R.; Hsu, M. A.; Scarborough, R. M. Inhibition of fibrinogen binding to GP IIb-IIIa by a GP IIIa peptide. *J. Biol. Chem*. **1991**, *266*, 1415−1421.
(26) Bajt, M. L.; Ginsberg, M. H.; Frelinger, A. L., 3rd; Berndt, M. C.; Loftus, J. C. A spontaneous mutation of integrin alpha IIb beta 3 (platelet glycoprotein IIb-IIIa) helps define a ligand binding site. *J. Biol. Chem*. **1992**, *267*, 3789−3794.

(27) Lanza, F.; Stierle, A.; Fournier, D.; Morales, M.; Andre, G.; Nurden, A. T.; Cazenave, J. P. A new variant of Glanzmann's thrombasthenia (Strasbourg I). Platelets with functionally defective glycoprotein Iib-IIIa complexes and a glycoprotein IIIa 214Arg- - - -214Trp mutation. *J. Clin. Invest.* **1992**, *89*, 1995−2004.

(28) Scheibler, L.; Mierke, D. F.; Bitan, G.; Rosenblatt, M.; Chorev, M. Identification of a contact domain between echistatin and the integrin $\alpha_v\beta_3$ by photoaffinity cross-linking. *Biochemistry* **2001**, *40*, 15117−15126.

(29) Miller, M. D.; Kearsley, S. K.; Underwood, D. J.; Sheridan, R. P. FLOG: a system to select quasi-flexible ligands complementary to a receptor of known three-dimensional structure. *J. Comput.-Aided Mol. Des.* **1994**, *8*, 153−174.

(30) Feuston, B. P.; Miller, M. D.; Culberson, J. C.; Nachbar, R. B.; Kearsley, S. K. Comparison of Knowledge-Based and Distance Geometry Approaches for Generation of Molecular Conformations. *J. Chem. Inf. Comput. Sci.* **2001**, *41*, 754−763.

(31) BatchMin and MacroModel were developed in the laboratories of Professor Clark Still (Columbia University) and are available from Schrodinger, Inc. (Portland, OR). Version 5.0 was released in 1995.

(32) Halgren, T. A.; Merck Molecular Force Field. I Basis, Form, Scope, Parametrization, and Performance of MMFF94, *J. Comput. Chem.* **1996**, *17*, 490−519

(33) Hunter, C. A.; Sanders, J. K. M.; The Nature of $\pi-\pi$ Interactions. *J. Am. Chem. Soc.* **1990**, *112*, 5525−5534.

(34) Xiong, J−P.; Stehle, T.; Zhang, R.; Joachimiak. A.; Frech, M.; Goodman, S. L.; Arnaout, M. A. Crystal structure of the extracellular segment of integrin $\alpha_v\beta_3$ in complex with an Arg-Gly-Asp ligand. *Science* **2002**, *296*, 151−155.

(35) Gottschalk, K. E.; Gunther, R.; Kessler, H. A Three-State mechanism of Integrin Activation and Signal Transduction for Integrin $\alpha_v\beta_3$. *ChemBioChem* **2002**, *5*, 470−473.

JM0203130